

# Modeling and simulation of high-power broad-area semiconductor lasers with optical feedback from different external cavities

(Invited Paper)

M. Radziunas\*, U. Bandelow\*, C. Bree\*, V. Raab†, H. Wenzel‡ and A. Zeghuzi‡

\*Weierstrass Institute, Mohrenstrasse 39, 10117 Berlin, Germany. Email: Mindaugas.Radziunas@wias-berlin.de

†Raab-Photonik GmbH, Amundsenstrasse 10, 14469 Potsdam, Germany.

‡Ferdinand-Braun-Institut, Leibniz-Institut für Höchstfrequenztechnik, Gustav-Kirchhoff-Str. 4, 12489 Berlin, Germany.

**Abstract**—We apply a dynamic (1+2)-dimensional traveling wave model and a corresponding parallel optoelectronic solver for simulations of broad-area semiconductor lasers. To avoid a significant slow-down of the numerical simulations in the presence of an external cavity, we perform a time-efficient modeling of the optical feedback. Finally, we present several simulated examples of parasitic optical feedback or an intended beam shaping by a specially designed external cavity.

Semiconductor laser (SL) diodes with optical feedback from external cavities (ECs) are experimentally and theoretically extensively studied dynamical systems providing a vast variety of different steady and dynamic states. The majority of work on SL-EC systems are devoted to the study of single-lateral mode narrow-waveguide SLs. However, the large stripe (aperture) width of broad-area (BA) SL diodes leads to the support of multiple lateral optical modes. Proper modeling of the resulting spatiotemporal dynamics in BASL diodes, in this case, should be performed by at least 1 (time  $t$ ) + 2 (space  $xz$ ) - dimensional partial differential equations. The detailed experimental and theoretical study of BASL-EC and high-power (HP) BASL-EC devices, in particular, becomes much more complicated. Due to potential applications of HP BASLs as high-power optical sources, the majority of work on HP BASL-EC systems studies the damages implied by unwanted reinjection of the optical fields or discusses methods for tailoring the emitted beam and improving the beam quality by optical feedback from a properly designed EC [1], [2]. To simulate the dynamics of BASLs, we use the traveling

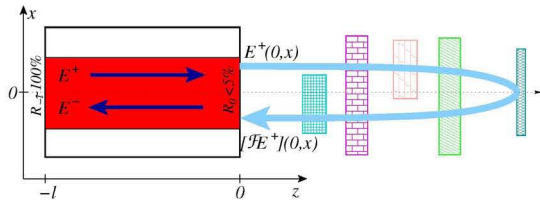


Fig. 1. Schematic representation of the broad-area laser diode with optical feedback from the external cavity containing different optical components such as lenses, (semitransparent) mirrors, Lyot- or photonic-crystal filters, or dispersive gratings.

wave (TW) model and the related parallel solver BALaser [3] developed at the Weierstrass Institute in Berlin and executed

on multicore compute servers there [4]. According to the TW model, the spatiotemporal evolution of the slowly varying complex amplitudes of two waves  $E^+(z, x, t)$  and  $E^-(z, x, t)$ , counterpropagating along the longitudinal axis ( $z$ -coordinate), is governed by the following TW equations,

$$\begin{aligned} \frac{1}{v_g} \partial_t E^\pm &= \left[ \mp \partial_z - \frac{i}{2k_0\bar{n}} \partial_{xx} - i\beta \right] E^\pm + F_{sp}^\pm, \\ E^+(-l, x, t) &= \sqrt{R_{-l}} E^-(-l, x, t), \\ E^-(0, x, t) &= \sqrt{R_0} E^+(0, x, t) + (1-R_0)[\mathcal{F}E^+](x, t). \end{aligned} \quad (1)$$

Here,  $v_g$ ,  $k_0 = 2\pi/\lambda_0$ ,  $\bar{n}$ , and  $F_{sp}^\pm$  are the group velocity of light, the free-space central wavenumber ( $\lambda_0$ : central wavelength), the reference refractive index, and the Langevin noise term, respectively. The complex propagation factor  $\beta(z, x, t)$  accounts for linear and nonlinear (two-photon) absorption [6], the initially induced refractive index profile, the material gain, and the refractive index. The last two factors depend on the excess carrier density and take into account nonlinear gain compression [6], material gain dispersion, and the static thermally-induced refractive index change [7].

A diffusive rate equation governs the dynamics of the carrier densities. Here, to determine carrier diffusion and injected current (pump) at the active zone, we simultaneously solve the carrier spreading problem in the lateral ( $x$ ) and vertical ( $y$ ) cross-sections of the BASL device [5]. Parameters  $R_{-l}$  and  $R_0$  are the intensity reflection coefficients at the (high-reflective) rear and (low-reflective) front facets  $z = -l$  and  $z = 0$ , respectively, of the diode ( $l$ : the length of the BASL), see Refs. [4], [6] for more details on the model and typical diode parameters.

Assuming that the beam collimation along the fast axis ( $y$  direction) is perfect, the optical feedback  $\mathcal{F}$  in the last row of Eq. (1) can be given as a general linear integral operator,

$$[\mathcal{F}E^+] = \int_{-\infty}^t \int_{\mathbb{R}} K(x', t', x, t) E^+(0, x', t') dx' dt', \quad (2)$$

where the kernel function  $K(x', t', x, t)$  depends on the configuration of the EC. For its construction, we exploit Huygens-Fresnel integrals within each optical element, see Fig. 1, and neglect the angular dependencies of optical path lengths.

For example, for a perfectly self-imaging EC (later referred to as EC<sub>1</sub>) containing two along the slow-axis ( $x$

direction) collimating (SAC) lenses this procedure implies  $K(x', t', x, t) = \eta\delta(x - x')\delta(t' - t + \tau)$ , where  $\delta$  is the Dirac delta function,  $\tau$  is the field roundtrip time in the EC, and  $\eta$  accounts for the field reflectivity at the mirror and the constant phase shifts at the lenses. For a perfect single SAC lens system providing an anti-symmetric self-imaging ( $EC_2$ ), this expression reads as  $K(x', t', x, t) = \eta\delta(x+x')\delta(t'-t+\tau)$  and can induce a more robust symmetricity of the emitted field. An implementation of both these spatially- and temporally-localized cases into our solver is uncomplicated and does not affect the numerical performance of the solver.

An introduction of any offsets in the positions of the optical elements induce perturbations of the operator  $K$  and makes the feedback term nonlocal in space, which can significantly violate the performance efficiency of our algorithm. This is because an evaluation of the feedback term within each time iteration is equivalent to the matrix-vector multiplication, in general requiring  $\sim N_x^2$  arithmetic operations ( $N_x$ : number of lateral domain discretization steps). Fortunately, numerically this problem can be handled by exploiting several computationally-cheap ( $\sim N_x \log(N_x)$  operations) fast Fourier transforms allowing easy switching between lateral ( $x$ -space) and angular ( $k_x$ -space) representations of the beam propagating along the optical axis.

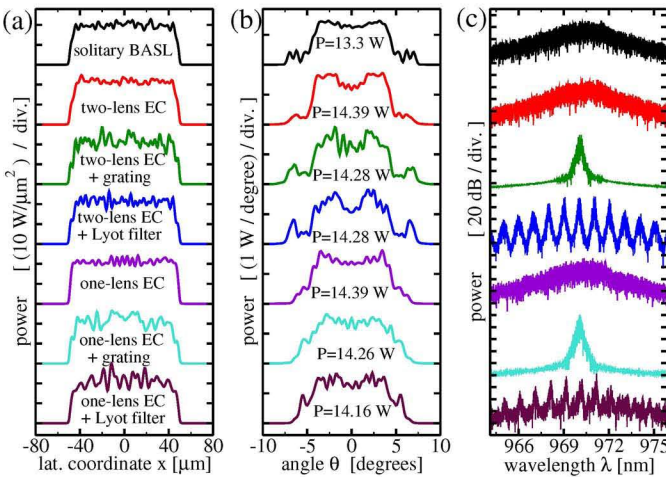


Fig. 2. Simulated time-averaged near fields (a), far fields (b), and optical spectra (c) of a 4 mm-long and 100  $\mu\text{m}$ -wide stripe BASL. Different curves in each panel counting them from the top represent solitary BASL, BASL with a simple EC<sub>1</sub> ( $\tau = 0.67$  ns,  $\eta = 0.2$ ), EC<sub>1</sub> with the diffractive grating filter, EC<sub>1</sub> with the Lyot filter, BASL with a simple EC<sub>2</sub> ( $\tau = 0.33$  ns,  $\eta = 0.2$ ), EC<sub>2</sub> with the diffractive grating filter, and EC<sub>2</sub> with the Lyot filter, respectively. The corresponding output power  $P$  are indicated in panel (b).

An introduction of more complex optical filtering elements (gratings, Lyot- or photonic crystal filters, for example) can also make the operator  $K$  nonlocal not only in space but in time as well, which, in general, is not affordable for our solver. To save the efficiency of our algorithm in these cases, we should approximate more precise beam propagation models by some simpler models admitting an efficient numerical performance. For example, the field scattering from a grating can be approximated by a Lorentzian in the frequency domain

and efficiently implemented by an infinite impulse response digital filter in simulations. Similarly, we approximate the action of the frequency-periodic Lyot-filter by a numerically inexpensive digital finite impulse response filter. Simulations of HP BASL alone and with the optical fields from several perfectly-allocated ECs with or without additional frequency-filtering elements are shown in Fig. 2. We note that the frequency filtering does not imply a significant reduction of the emission power. Due to nonvanishing optical feedback in the BASL-EC devices, the emission intensity at the diode facet is slightly higher compared to the solitary BASL.

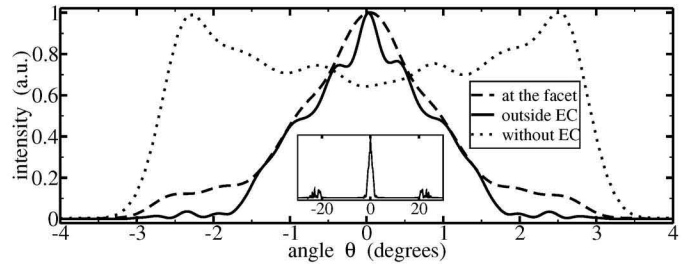


Fig. 3. Simulated ( $\sim 3$  W) emission of the 1 mm-long and 100  $\mu\text{m}$ -wide stripe BASL with optical feedback from the EC containing an optimized chirped photonic crystal filter. Dashed: time-averaged Fourier transformed near field at BASL output facet. Solid: far-field coupled out from EC. Dotted: BASL emission without EC. Insert: same, on a larger angular scale.

Considering a photonic crystal filter acting in the angular domain, we exploit a model based on a non-paraxial beam propagation method. In this case, a matrix-vector multiplication performed in the  $k_x$ -domain is numerically affordable due to a few-diagonal structure of the transfer matrix [2]. An example of the simulated shaping of the far-fields of a 1mm-long HP BASL with specially tailored EC is shown in Fig. 3. The angular filtering (cf. dotted and solid curves) is achieved for a nonvanishing dislocation of the laser facet and the focal plane of the (single) SAC lens. For more details, see Ref. [2].

To conclude, we have discussed dynamical modeling of HP BASL-EC devices. The optical feedback model, in general, should be separately derived for each EC. Models for several types of ECs were implemented into our dynamic optoelectronic solver, and example simulations were presented.

#### ACKNOWLEDGMENT

This work is supported by the EUROSTARS Project E!10524 HIP-Lasers and by the German Federal Ministry of Education and Research contract 13N14005 as part of the EffiLAS/HotLas project.

#### REFERENCES

- [1] V. Raab and C. Raab, *Zeitschrift Photonik*, **5**(5), 46–49, 2004.
- [2] C. Brée et al., submitted to *Journal of Optics*, available as a WIAS-Preprint 2502, 2018.
- [3] “BALaser: a software tool for simulation of dynamics in Broad Area semiconductor Lasers,” <http://www.wias-berlin.de/software/BALaser>.
- [4] M. Radziunas, *The Int. J. of High Perform. Comp. Appl.*, First online December 23, 2016, doi: 10.1177/1094342016677086.
- [5] M. Radziunas et al., *Optical and Quantum Electronics*, **49**, 332, 2017.
- [6] A. Zeghzu et al., *Opt. and Quantum Electron.*, **50**, 88, 2018.
- [7] S. Rauch et al., *Appl. Phys. Lett.* **110**(26), 263504, 2017.